ORIGINAL RESEARCH ARTICLE





Climate and Vegetation Change in a Coastal Marsh: Two Snapshots of Groundwater Dynamics and Tidal Flooding at Piermont Marsh, NY Spanning 20 Years

Sofi Courtney^{1,2} · Franco Montalto³ · Elizabeth Burke Watson^{1,4}

Received: 17 July 2023 / Accepted: 5 December 2023 © The Author(s), under exclusive licence to Society of Wetland Scientists 2023

Abstract

Groundwater hydrology plays an important role in coastal marsh biogeochemical function, in part because groundwater dynamics drive the zonation of macrophyte community distribution. Changes that occur over time, such as sea level rise and shifts in habitat structure are likely altering groundwater dynamics and eco-hydrological zonation. We examined tidal flooding and marsh water table dynamics in 1999 and 2019 and mapped shifts in plant distributions over time, at Piermont Marsh, a brackish tidal marsh located along the Hudson River Estuary near New York City. We found evidence that the marsh surface was flooded more frequently in 2019 than 1999, and that tides were propagating further into the marsh in 2019, although marsh surface elevation gains were largely matching that of sea level rise. The changes in groundwater hydrology that we observed are likely due to the high tide rising at a rate that is greater than that of mean sea level. In addition, we report changes in plant cover by *P. australis*, which has displaced native marsh vegetation at Piermont Marsh. Although *P. australis* has increased in cover, wrack deposition and plant die off associated Superstorm Sandy allowed for native vegetation to rebound in part of our focus area. These results suggest that climate change and plant community composition may interact to shape ecohydrologic zonation. Considering these results, we recommend that habitat models consider tidal range expansion and groundwater hydrology as metrics when predicting the impact of sea level rise on marsh resilience.

Keywords Groundwater hydrology · Eco-hydrological zonation · Marsh macrophyte · Climate change · Sea level rise · Coastal wetland

Sofi Courtney sofifrancescourtney@gmail.com

- Department of Biodiversity, Earth & Environmental Sciences, Patrick Center for Environmental Research, The Academy of Natural Sciences, Drexel University, Philadelphia, PA, USA
- Present address: School of Environmental and Forest Sciences, University of Washington, Seattle, WA, USA
- Department of Civil, Environmental, and Architectural Engineering, Drexel University, Philadelphia, PA, USA
- Present address: Department of Ecology and Evolution, Stony Brook University, Stony Brook, NY, USA

Introduction

Groundwater hydrology plays an important role in coastal marsh biogeochemical and ecological function (Nuttle and Hemand 1988; Harvey and Odum 1990; Allen 2000; Montalto and Steenhuis 2004; Charette 2007; Wilson and Morris 2012; Shi et al. 2019; Guimond et al. 2020a), in large part because groundwater dynamics drive the zonation of marsh macrophyte community distribution (Moffett et al. 2012; Cao et al. 2012; Xin et al. 2013; Wilson et al. 2015b; Moffett and Gorelick 2016; Xie et al. 2020). Temporal dynamics such as sea level rise (SLR), shifts in plant community composition, and climate change are altering marsh groundwater dynamics.

(Smith and Medeiros 2013; Wang et al. 2017; Knott et al. 2019; Guimond et al. 2020a) which consequently changes marsh macrophyte habitat suitability and spatial zonation

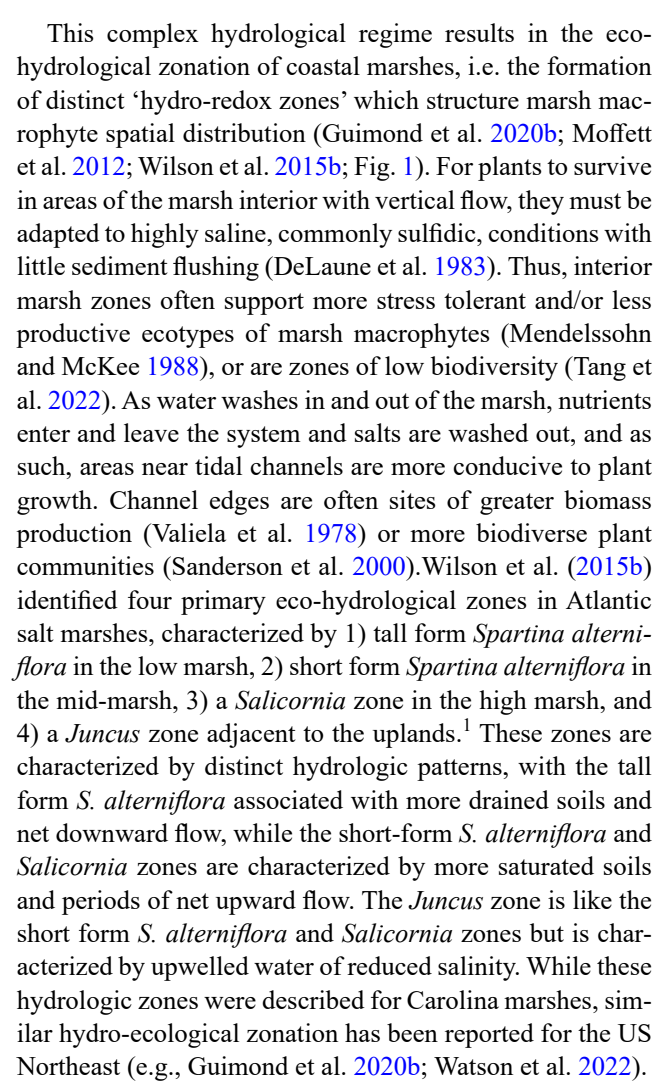


8 Page 2 of 17 Wetlands

(Chui et al. 2011; D'Alpaos and Marani 2016; White and Madsen 2016; Guimond et al. 2020b) and is likely contributing to marsh loss due to marsh macrophyte die-back (Smith et al. 2012; Hughes et al. 2012). However, while there has been extensive investigation of how groundwater impacts spatial dynamics in marshes, there is little research into how groundwater function changes over time in the context of shifting environmental conditions. This study addresses this gap in scientific knowledge by examining both spatial and temporal changes in hydrology and plant species distribution at a brackish tidal marsh in the Hudson River Estuary.

Major hydrological influences on coastal marshes are (semi-)diurnal tides, groundwater flow from terrestrial uplands, precipitation, and evapotranspiration (Xin et al. 2017). Tides produce daily fluctuations in groundwater table elevation as seawater is forced into and drains out of the marsh platform through tidal creeks. While the mean marsh water table is near the marsh surface, at high tides areas of the marsh may flood and at low tides water may only flow subterraneously (Xin et al. 2022). The amplitude of tidally influenced groundwater fluctuations in each marsh is determined by the tidal range, the hydraulic conductivity of the marsh sediments and creek morphology. For instance, coastal areas with a greater tidal range and sediments with high conductivity allow water to flow faster and further into the marsh platform. The morphology of tidal creeks influences subsurface flow due to gravitational forces. Creeks with steep banks push more water into marshes at high tide and flush out more completely at low tide because of the steep tidal gradient to the marsh interior (Mazda and Ikeda 2006).

Due to the restricted length of a tidal period and the low permeability of marsh sediments, water exchange through the marsh platform decreases with distance from tidal creeks (Harvey and Odum 1990; Williams et al. 2002; Wilson et al. 2011; Watson et al. 2022). Generally, the marsh platform at the creek edge is flooded and drained during each tidal cycle, resulting in fluctuations in water table elevation and tidal-groundwater exchange (Montalto et al. 2006; Watson et al. 2022). The water table elevation in the marsh interior is primarily driven by terrestrial groundwater inputs, precipitation, evapotranspiration, and neap and spring tides. Freshwater flows into the marsh from the terrestrial uplands and converges with saltwater inputs tidally forced from ocean systems. This flow convergence results in an upward flow, i.e. vertical forcing (Wilson et al. 2015b). This results in a relatively high water table in the marsh interior which rarely drains, so salts produced during evaporation and biological processes are not flushed out of the sediment. Consequently, the groundwater in the high marsh is higher in elevation and relatively saline compared to the creek edges (Xin et al. 2022).



While conventional evaluations of wetland susceptibility to SLR have primarily focused on wetland elevation change or using modeled biophysical feedbacks to predict ecosystem state changes (Raposa et al. 2016; Cole Ekberg et al. 2017; Elsey-Quirk et al. 2022), this study investigates alterations in the marsh's groundwater table and the impact of tides by utilizing historical data to evaluate temporal changes. Understanding how eco-hydrologic zonation is evolving with increasing sea level is an important research question. On one hand, modeling studies have suggested that relative SLR will initially cause the poorly aerated interior groundwater zone to contract considerably (Xin et al. 2022), and positive SLR anomalies in Massachusetts have been positively correlated with increased plant biomass production (Morris et al. 2013). However, other work suggests that once the marsh platform is excessively inundated, sediment flushing will likely decrease (Wilson et al. 2015a; Guimond



¹ A revision of the *Spartina* genus, recognized by most floras, has led to renaming of *Spartina alterniflora* to *Sporobulous* alterniflorus and *Spartina patens* to *Sporobulous pumilus*.

Wetlands Page 3 of 17 8

et al. 2020b; Guimond and Tamborski 2021). In addition, there is widespread evidence that poorly drained areas in the upper marsh are expanding across the US Atlantic Coast leading to widespread loss of high marsh plant taxa (Smith et al. 2013; Smith 2015; Raposa et al. 2017; Rippel et al. 2023) and the formation of bare areas in the upper marsh (Watson et al. 2017; Schepers et al. 2020). Thus, documenting how the water table has evolved in situ at a marsh over the last two decades with SLR and in concert with vertical elevation change is of considerable interest.

A potentially confounding factor in this study is the effect of the invasion of *Phragmites australis*. Piermont Marsh is a mesohaline marsh (5–10 psu) (Yozzo and Osgood 2013), and as such is vulnerable to P. australis invasion. Examination of the area of *P. australis* at Piermont marsh (Lathrop et al. 2003) found it present, but at low abundances from 1965 to 1980 (<15%). After 1980, it expanded to cover 60–70% of the marsh in the 1990s to approximately 90% by 2013. Marsh plants are known to influence the water table through evapotranspiration (Dacey and Howes 1984; Moffett et al. 2012; Xin et al. 2017), and to even help create eco-hydrologic zonation due to varied evapotranspiration rates, root penetration profiles, and salinity zones (Moffett et al. 2012). In this case, although studies report varied evapotranspiration rates, high plant coefficients (the ratio of evapotranspiration to pan evaporation) are consistently reported for *P. australis* in comparison with salt marsh species more generally (Borin et al. 2011; Milani and Toscano 2013), with daily rates of evapotranspiration that average 2-9 mm (Burba et al. 1999; Zhou and Zhou 2009; Headley et al. 2012; Anda et al. 2017). Thus, if P. australis invaded our study transect after 1999, we may expect its increased presence to reduce water table levels, especially during the spring and early summer growing season (Fig. 1).

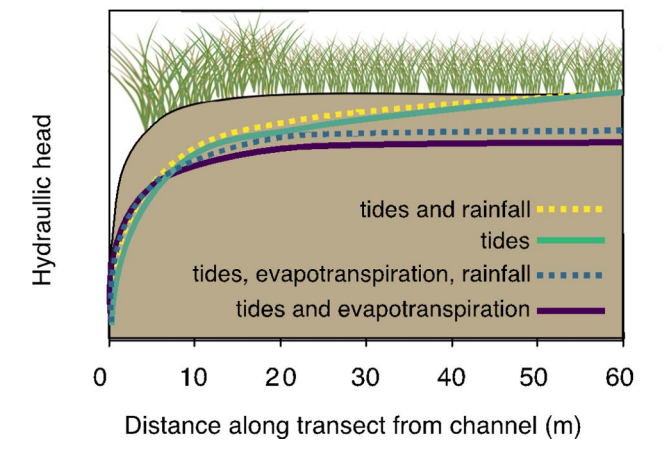


Fig. 1 Comparison of the annually averaged hydraulic head across a marsh transect perpendicular to a tidal channel. Simulations were based on realistic values for tides, precipitation, rainfall, and evaporation. Precipitation puts the water table at a shallower depth, while evapotranspiration deepens it. Adapted from Xin et al. 2017

The goal of this study was to quantify how the marsh water table has evolved over a 20-year period at Piermont Marsh, just outside of New York City, in response to SLR acceleration, and potentially in combination with *P. australis* invasion. In 1999 Montalto et al. (2006) mapped the hydrology of a brackish tidal marsh within the Hudson River estuary by assessing a variety of variables including topography, water table elevation, and hydroperiod and found low levels of tidal influence and an increase in water table elevation within the marsh interior. Twenty years later this study revisited the site and methods used by Montalto et al. to evaluate the change in marsh hydrology over time due to SLR and its relation to marsh macrophyte distribution. We installed and instrumented groundwater wells along a transect perpendicular to a large tidal creek, at locations nearly identical to their position 20 years earlier (Montalto et al. 2006), measured water levels through the spring months, and conducted topographic surveys. We additionally examined tide gauge data from the Battery, NY, to help contextualize these values relative to astronomical cycles (the 18.6 lunar nodal cycle and 8.85 lunar perigee cycle), and analyzed vegetation change maps to understand the potential role of P. australis invasion in shaping groundwater dynamics.

Materials and Methods

Study Site

Piermont Marsh is a 417-hectare tidal marsh located within the Hudson River Estuary in New York, United States (Fig. 2) which experiences diurnal mesohaline tides and is bisected by tidal creeks and channels. The marsh is located at the southernmost edge of the Hudson River National Estuarine Research Reserve (HRNERR) and is designated as a Significant Coastal Fish and Wildlife Habitat by the New York State Department of State (NYDOS 2012) and a Critical Environmental Area by Piermont Village (NYS-DEC 1985). The site's vegetation is dominated by P. australis but retains some small patches of native marsh species in the interior. Local land managers and residents anecdotally report that species diversity on the marsh has decreased over the last few decades (NYSDEC 2017). Salinity typically ranges from 3% during spring to 10% during summer (Osborne et al. 2015).

Study Design

Hydrologic measurements were collected over the summer of 2019 on Piermont Marsh. These data were compared to hydrological measurements made in 1999, which focused on describing the marsh water elevation across a transect



8 Page 4 of 17 Wetlands

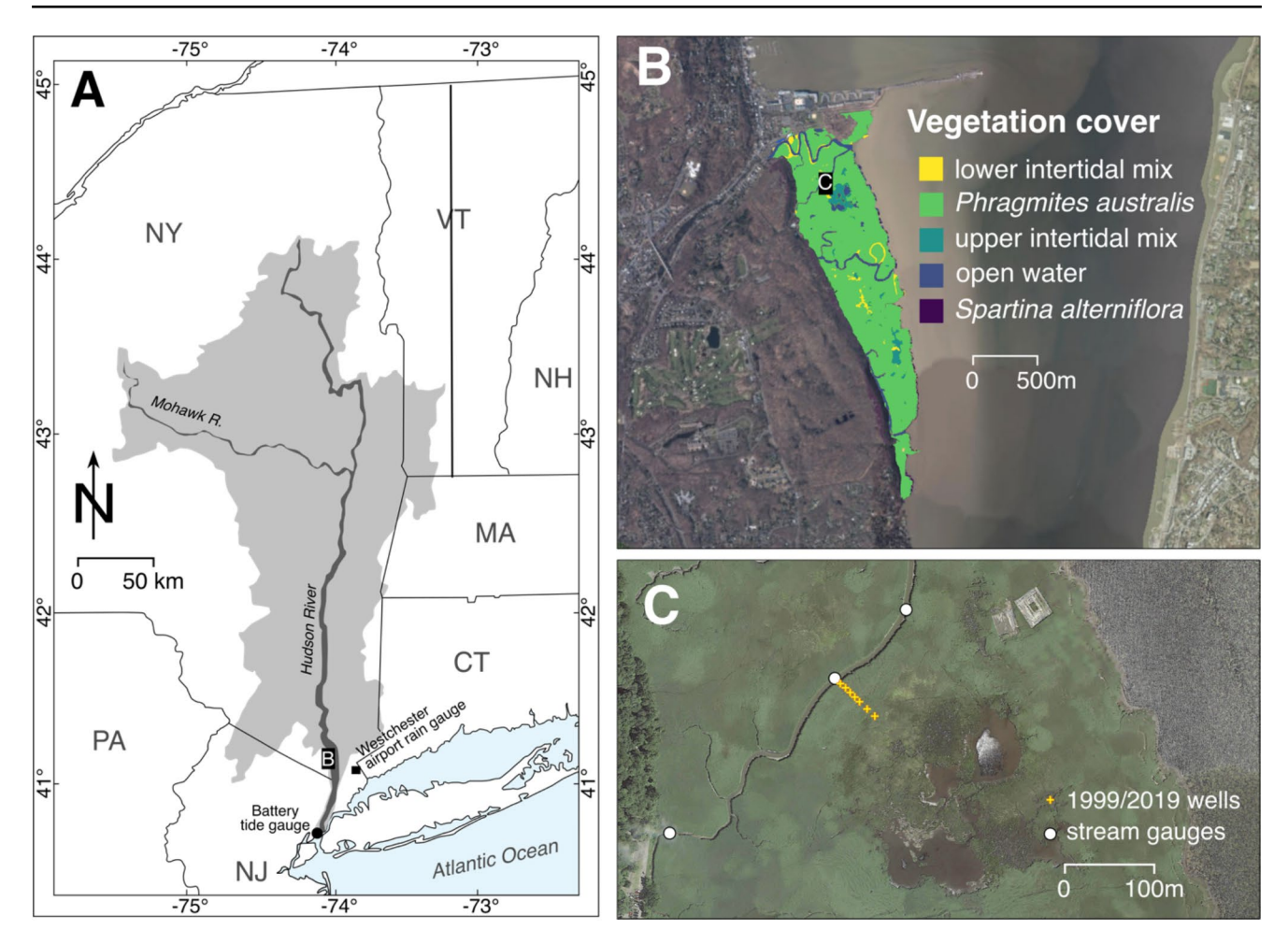


Fig. 2 Map of study area showing (a) the Hudson River Valley with the location of Piermont Marsh; (b) Vegetation cover at Piermont Marsh in 2014 (provided by the HRNERR) which is dominated by the nonnative *Phragmites australis*; (c) the location stream gauges (denoted

from a large tidal channel to the marsh interior (Montalto et al. 2006). The aim of this study was to compare current tidal flooding and groundwater table levels with measures made in 1999, to compare tidal hydrology at these two time points which are quite distinct in terms of marsh and water level elevations (Fig. 3).

Water Table Measurements

To determine ground water levels and tidal flooding throughout the marsh, seven water level loggers were installed along a gradient from the tidal channel to the upland, replicating the measures conducted by Montalto et al. (2006) (Fig. 2). The locations of Montalto's wells were established by georeferencing maps from Montalto et al. 2006 using Google Earth (ver. 7.3.2.5776) and were confirmed visually by Montalto in the field. Wells were constructed by suspending a pressure transducer within a 7.5 cm diameter perforated PVC pipe lined with screening to prevent sediment from as circles) as well as groundwater wells along the a transect perpendicular to a tidal channel and in two areas of expanding ponded water at Piermont Marsh. The location of map insets (marked 'b' on map a and 'c' on map b) is shown

entering the well. The wells sat 1-m below the marsh surface, 0.6 m above the soil surface, was vented to the atmosphere, and only the length below soil was perforated. A concrete collar was installed at the marsh surface around the well to prevent the preferential flow of water down the side of the well. Seven wells were installed along the original transect, perpendicular to the creek (Fig. 2).

Wells were installed 5 May 2019 and well water levels were monitored from 5 May 2019–30 June 2019. We were not able to match the exact timeline of 1999 observations, but we compare 5 May – 30 June of 2019 with 6 April – 26 May of 1999. The absolute elevation of the top of each well was measured using RTK-enabled static GPS measurements from Leica GNSS GS14 rover units and static measures using an AX1202 GG base station unit to reference water levels to the NAVD88 vertical datum. Reference water levels were measured each time data was collected, as the distance of the top of the well to the water surface, which using the well-top elevations was convert to elevation relative to



Wetlands Page 5 of 17 8

Table 1 Locations and monitoring information for 1999 and 2019 water level monitoring. The location for groundwater wells indicates distance from the tidal channel. The 2019 well data was compared with well data collected along the same transect 6 April 1999-26 May 1999

Creek distance (m)	Latitude	Longitude	1999 elevation (m)	2019 elevation (m)	Elevation change (cm)	Elevation change (mm yr ⁻¹)	2019 deployment
0	41.03606°	-73.91050°	0.61	0.72	11± 3 cm	5.5 ± 1.7	5 May – 30 June 2019
6	41.03602°	-73.91046°	0.63	0.72	9 ± 3 cm	4.5 ± 1.7	5 May - 30 June 2019
12	41.03598°	-73.91041°	0.64	0.73	9 ± 3 cm	4.5 ± 1.7	5 May – 30 June 2019
18	41.03594°	-73.91036°	0.65	0.75	10 ± 3 cm	5.0 ± 1.7	5 May – 30 June 2019
24	41.03590°	-73.91032°	0.66	0.77	11 ± 3 cm	5.5 ± 1.7	5 May – 30 June 2019
36	41.03581°	-73.91023°	0.68	0.72	4 ± 3 cm	2.0 ± 1.7	5 May - 30 June 2019
48	41.03572°	-73.91014°	0.69	0.80	11 ± 3 cm	5.5 ± 1.7	5 May - 30 June 2019

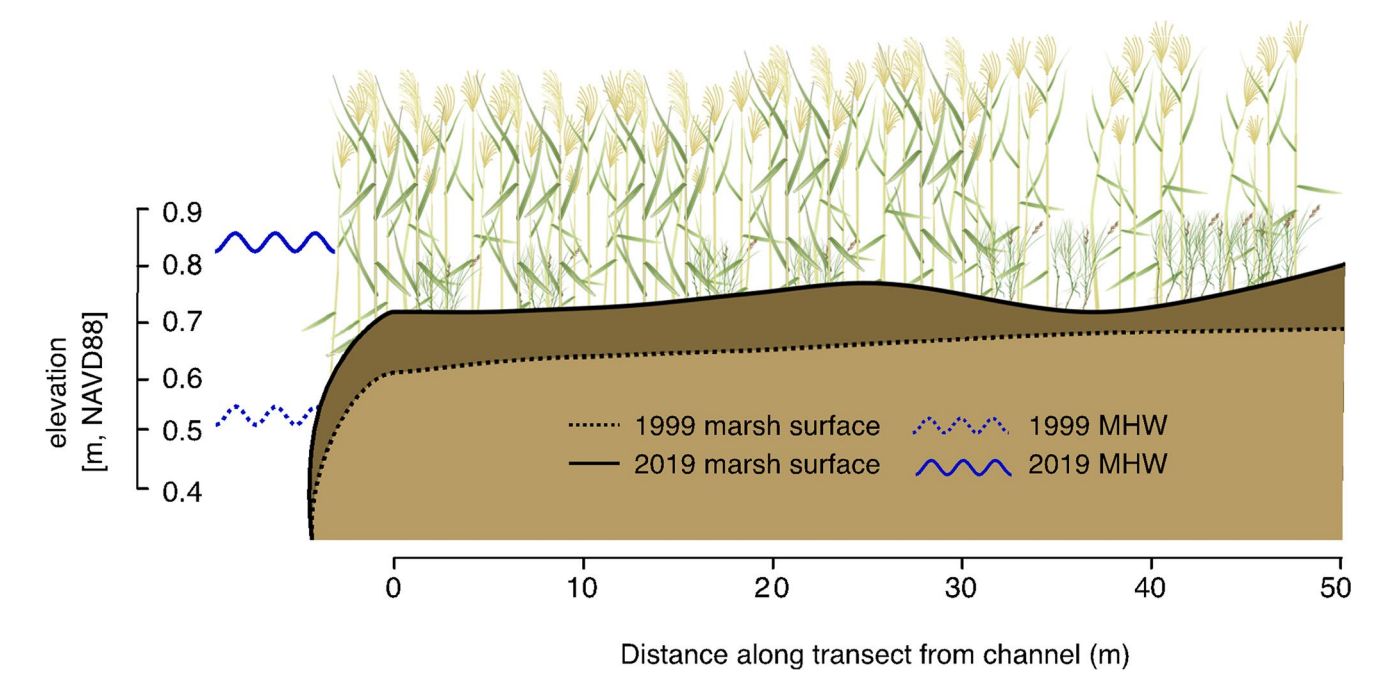


Fig. 3 Marsh elevation across the studied transect at Piermont Marsh between 1999 and 2019, also showing the mean high water (MHW) calculated for channel loggers deployed in 1999 and 2019 (5 May –12 Aug). The section of the transect that appears to have not

the NAVD88 datum. To relate marsh elevation with water elevations, GPS surveys were also conducted along the transect using a Leica GNSS GS14 rover unit. Elevation control for the 1999 wells and water levels were similarly measured with survey-grade GPS, which was unusual for the time, and which permits the level of comparison achieved by this study. We report on marsh elevation change (Table 1), which we report as the difference in marsh elevation at well locations between 1999 and 2019. In addition to measuring water levels at Piermont Marsh, we also downloaded and analyzed data from the Battery tide gauge for these same time periods (NOAA 2023).

There is a sometimes a significant lag in response times for wells or piezometers with large diameter or narrow screened intervals (Gardner 2009). As this lag can cause large deviations between the aquifer head and measured

increased in elevation significantly overlaps with the area that experienced dieback after Hurricane Sandy, likely due to wrack deposition. Icons obtained courtesy of: https://ian.umces.edu/media-library/phragmites-australis-common-reed-singular/

water table, we calculated the well time constant (T_c) according to equation one, where:

$$T_c = \frac{R^2}{K_s L} \tag{1}$$

R is the well diameter, K_s is the saturated hydraulic conductivity, and L is the screened interval. For these calculations, we used mean saturated hydraulic conductivity of 7.75×10^{-3} cm s⁻¹, measured by Montalto et al. (2006).

Analysis of Environmental Drivers

Changes in the marsh water table were compared with important potential hydrologic and vegetation changes that have occurred over the past 20 years. We calculated rates



of change in monthly water levels at the Battery, NY for the 1999-2019 period using two different methods. We modeled change over time in monthly highest water levels, mean high water (MHW), mean tide level (MTL), and mean low water (MLW) using an ordinary least squares regression model with ARIMA errors to account for the autoregressive structure of tide data, after first removing the annual cycle using a curve with a 1-yr periodicity (Foster and Brown 2015). The ARIMA errors model was fit using the function auto.arima using the package forecast (Hyndman and Khandakar 2008). We calculated the squared correlation of fitted to actual values to produce a pseudo- r^2 . For comparison, we calculated trends generated using ordinary least squares regression for the 1999-2019 period, although it is likely that the temporal autocorrelation causes uncertainty to be underestimated. Data and reproducible code for this procedure can be found as supplemental material the Dryad Digital Repository.

We obtained vegetation maps from the HRNERR from 1997, 2005, 2014, and 2018 to help determine change over time in the coverage of plant species, which may alter evapotranspiration and water table patterns (NYSDEC 2023). A 20-m buffer was located around each of the points where wells were located, and the composition of the vegetation in this buffer zone was quantified using QGISver. 3.30.2. Four time points is generally not sufficient for statistical identification of trends (Yue et al. 2002), but changes were interpreted.

Representativeness of Sampling Periods

To contextualize the time period of measures (i.e., to ensure that our chosen seasons were not anomalous), we used the Battery tide gauge data to compare water levels in spring 1999 and 2019 relative to astronomical cycles that drive interannual sea level variability, and we compared spring high tide levels in 1999 and 2019 with surrounding years. The principal astronomical cycles thought to influence tides include the 18.6 year lunar nodal cycle, and the 4.4 year subharmonic of the 8.85 year lunar perigee cycle (Haigh et al., 2011). Because our 1999 and 2019 measures were collected in slightly different time periods (April/May 1999 vs. May/ June 2019), we also examined mean monthly water levels (1980–2022) from the NOAA Battery tidal gauge to identify potential artifacts (NOAA 2023). We obtained rainfall data from spring of 1999 and 2019 from the nearest precipitation monitoring station (Westchester airport) to determine whether measures were made during an usually wet or dry period (NCEI 2023). The sampling periods were 20 years apart so they took place at approximately at the same point in the 18.6 year lunar nodal cycle.



Pressure transducer data was post-processed using HOBOware Pro (Ver. 3.7.16, Onset Computer Corporation, Bourne, MA) using reference water levels collected in the field and were corrected for atmospheric pressure using the HOBOware barometric compensation assistant, using data from the Hudson River National Estuarine Research Reserve (NERRS 2019).

Raw water elevation data from 1999 was analyzed in concert with the 2019 data. Water level data from 1999 were converted from the NVGD29 to NAVD 88 datum using NOAA VDatum v4.0.1 (NOAA 2019) prior to analysis. The transducer in well seven experienced three brief malfunctions from 30 May to 3 June 2019, which resulted in inaccurate elevation measurements for a total of 19.5 h. These data were excluded from the analysis. In 1999, Montalto also experienced malfunctions at the well 48 m from the creek. These data were corrected by Montalto into smoothed sixhour increments using average water elevation measurements and calculated error and calibrated using regression (Montalto et al. 2006). No other well transducers appeared to have malfunctioned.

Changes in surface flooding were estimated tide gauges installed at Piermont Marsh in 1999 and 2019 (5 May - 12 August). Marsh flooding was calculated as the percentage of time that water levels exceeded the average marsh elevation (0.75 m NAVD in 2019 and 0.65 m NAVD in 1999). The number of tides that flooded the marsh per month and the average maximum flooding depth were identified for 1999 and 2019. However, because the 1999 tide gauge was not operational for most of the period that the well loggers were collecting data for, we also utilized data from the NOAA tide gauge located at the Battery, NYC, 55 km distance (for plotting purposes and tidal efficiency calculations, described below), recognizing that the tidal regimes would not completely match. We used the Wilcoxon rank sum test to determine whether there were statistically significant differences in central tendency and the F variance test to analyze for statistically significance differences in variance between 1999 and 2019 for the marsh ground water levels at high and low tide. We partitioned the data by spring and neap tidal cycles, considering both depth relative to the marsh surface as well as elevation relative to the NGVD88 datum.

Tidal efficiency (*TE*) is defined as the ratio of the amplitude of the water level fluctuation in an inland well (s_w) to the corresponding amplitude of sea level fluctuation (s_w) (Van der Kamp 1972; Jiao and Post 2019), and while it is generally utilized to examine horizontal movements of tides in a confined coastal aquifer, here we adapted this metric to examine change over time in groundwater fluctuations.



Wetlands Page 7 of 17 8

Tidal efficiency (*TE*) was calculated for 1999 and 2019 well data empirically according to Eq. 2 as:

$$TE = \frac{s_w}{s_t} \tag{2}$$

where s_w is the daily range of water-level fluctuation in a well tapping the groundwater table and s_t refers to the daily range of tide (Ferris et al. 1962). TE was calculated based on the range of tide reported from the NOAA tide gauge at the Battery, NY. Tidal efficiency between years was compared using a two-sample Wilcoxon rank sum test.

To estimate uncertainty in water surface elevations and elevation change we conducted an error analysis that included uncertainty in GPS elevation surveys (2-cm) and water level accuracy (3-cm) based on manufacturer documentation, and conversion factors for NGVD29 vs. NAVD88 (2-cm) (Mulcare 2004). The error analysis was conducted using the quadratic sum for independent uncertainties (Taylor 1997). This uncertainty was then compared with measured differences.

Data visualization and analysis were performed in R 4.1.3 (R Core Team 2022) using packages dplyr (Wickham et al. 2022), forecast (Hyndman and Khandakar 2008), FSA (Ogle et al. 2023), ggplot2 (Wickham 2016), ggpubr (Kassambara 2023), ggsignif (Ahlmann-Eltze and Patil 2021), lmtest (Zeileis and Hothorn 2002), sandwich (Zeileis 2004; Zeileis et al. 2020), splines (Bates and Venables 2023) tseries (Trapletti and Hornik 2023), TTR (Ulrich 2021), and vioplot (Adler et al. 2022).

Results

Marsh Elevation

Marsh elevations increased at all stations at rates that ranged from 2.0 to 5.5 mm yr⁻¹ (Table 1). Generally, the elevation was highest in the marsh interior, and lowest adjacent to the tidal channel, in both 1999 and 2019. During both time periods, the marsh elevation was 0.08 m higher in the marsh interior than adjacent to the tidal channel and had a gentle upward slope. Mean high water measured at channel loggers was 0.52 m relative to the NAVD88 datum in 1999 and 0.87 in 2019. This increase, estimated at 1.6 cm yr⁻¹, is double the rate of increase in SLR measured at the Battery tide gauge (1.6 cm yr¹ vs. 0.82 cm yr¹; Table 2) and may be partly related to a deepened tidal channel that more effectively conveys tides (Fig. 3).

Vegetation Change and sea Level rise

Vegetation cover along the studied transect changed between 1997 and 2018, with salt meadow vegetation (e.g., high marsh species such as Spartina patens) declining near the tidal channel but persisting further inland. In 1997, the percent cover of salt meadow vegetation increased linearly across the transect, from 0.3% adjacent to the tidal channel, to 2.7% at 6-m, to 5.9% at 12-m, to 9.0% at 18-m, to 12.9% at 24-m, to 14.1% at 36-m, to 36.7% at 48 m. In 2018, the percentage of salt meadow vegetation cover was 0% adjacent to the channel, and at 6-m, 12-m, 18-m and 24-m. At 36-m the cover by salt meadow vegetation was 13.5%, and at 48-m it was 43.2% cover (Fig. 4). Superstorm Sandy, which affected the marsh in 2012, was associated with a large wrack deposit adjacent to the tidal channel (e.g., 20-30 m in from the tidal channel), which was responsible for increased bare ground in 2012–2014. Although by 2014, much of this wrack was no longer visible on aerial imagery, the area along the transect lacking in vegetation was still larger in 2014 than it was in 1997 or 2005. In summary, salt meadow vegetation persisted around the furthest stations (36 and 48 m) but was not apparent closer to the tidal channel, possibly due to the impact of Superstorm Sandy in 2012.

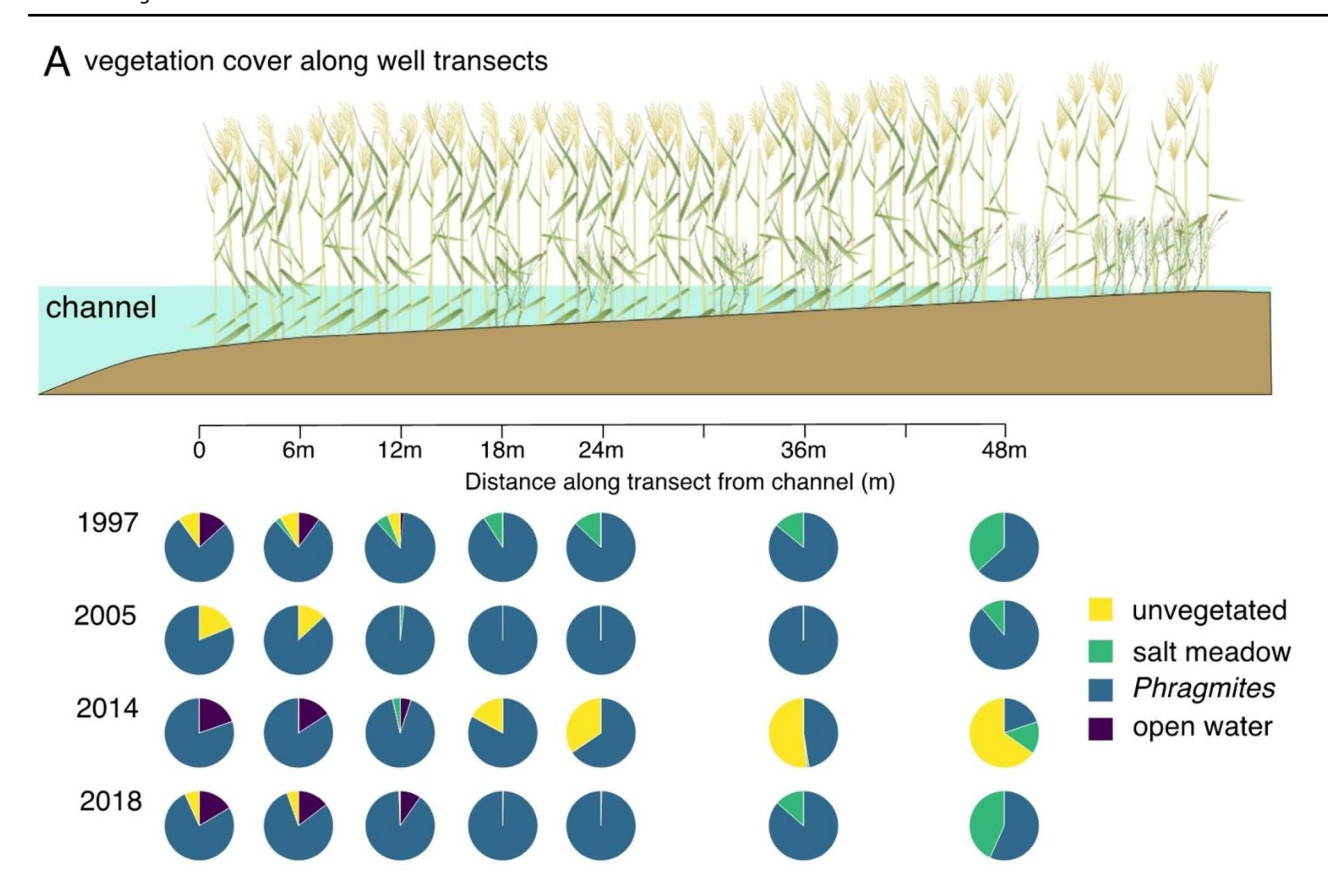
Trends in the rate of rise in mean sea level, mean tide level, mean high water and mean low water suggest significant increases in water levels have occurred in New York over the 20-year period centered on 1999–2019 (Table 2). Using ordinary least squares regression, we found an increase between 1999 and 2019 of monthly highest water at the NYC Battery tide gauge of 10 ± 2.2 mm yr⁻¹, an increase in monthly mean high water of 8.2 ± 0.97 mm yr⁻¹, an increase of monthly mean tide level of 5.6 ± 0.93 mm yr⁻¹, and an increase of monthly mean low water of 3.1 ± 0.95 mm yr⁻¹. These rates were similar to those found using linear models constructed with autoregressive and in some cases moving average terms, although ordinary least square modeling approach underestimates the uncertainty in the rate of change due to serial autocorrelation.

Marsh Water Levels

Comparing the channel gauge records with marsh elevations in 1999 and 2019 suggest that tidal flooding has increased. The average marsh elevation along the transect in which the wells were placed was flooded 3.2% of the time in 1999, and 9.9% of the time in 2019. In 1999, the marsh flooded on average 12 times per month between May and August. The average flooding duration was 2.1 ± 0.80 h (mean \pm standard deviation), and the marsh flooded on average to a depth of 8.7 ± 5.4 cm. In contrast in 2019, the marsh flooded on



8 Page 8 of 17 Wetlands



B trends in vegetation cover along well transect

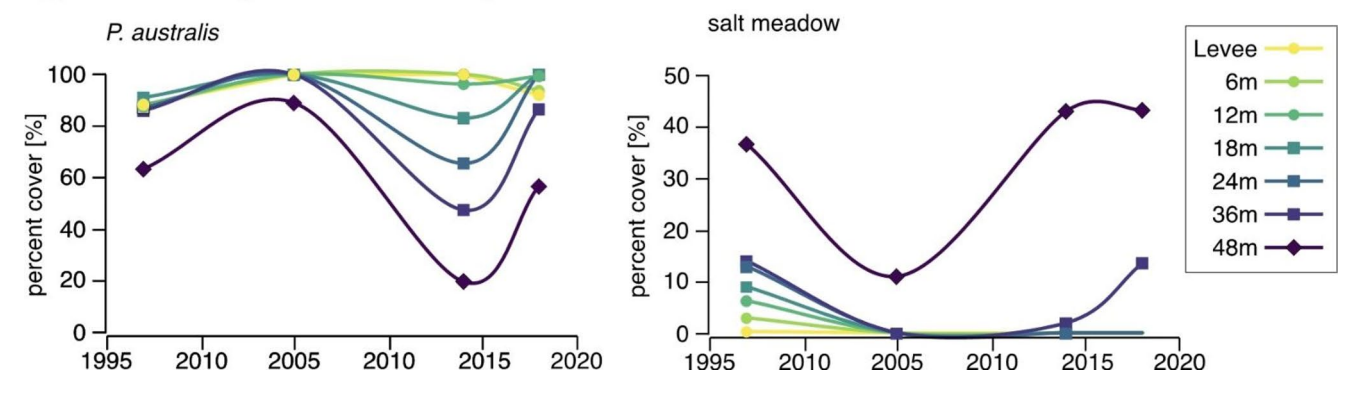


Fig. 4 Vegetation cover along a transect perpendicular to a tidal channel at Piermont Marsh showing (a) spatial patterns in plant cover during 1997, 2005, 2014, and 2018 (b) percent cover of *Phragmites australis*

and salt meadow during those same time periods. Density of vegetation reflects cover categories, with icons obtained courtesy of: https://ian.umces.edu/media-library/phragmites-australis-common-reed-singular/

Table 2 Rates of change and uncertainties in water level datums. Uncertainties are the standard error of the coefficient estimates. WL signifies monthly water level - highest, mean monthly high water (MHW), mean monthly tide level (MTL), or mean monthly low water (MLW). rWL signifies a residual water level after removing the modeled seasonal oscillation

Modeling approach	Highest $(\pm SE)$	MHW $(\pm SE)$	$MTL (\pm SE)$	$MLW (\pm SE)$
lm (WL~year)	$10 \pm 2.2 \text{ mm yr}^{-1}$ $r^2 = 0.081$ $p = 4.6 \text{ e}^{-0}6$	$8.2 \pm 0.97 \text{ mm yr}^{-1}$ $r^2 = 0.22$ $p = 2.3 \text{ e}^{-15}$	$5.6 \pm 0.93 \text{ mm yr}^{-1}$ $r^2 = 0.13$ $p = 5.3 \text{ e}^{-0.9}$	$3.1 \pm 0.95 \text{ mm yr}^{-1}$ $r^2 = 0.041$ p = 0.0013
auto.arima $(rWL \sim xreg = year)$	$10 \pm 2.4 \text{ mm yr}^{-1}$ pseudo- $r^2 = 0.092$ p = 2.4 e-05 ARIMA (1,0,0) errors	$7.5 \pm 1.5 \text{ mm yr}^{-1}$ pseudo- $r^2 = 0.47$ p = 1.2 e-06 ARIMA (2,0,3) errors	$5.5 \pm 1.3 \text{ mm yr}^{-1}$ pseudo- $r^2 = 0.33$ p = 3.7 e-05 ARIMA (2,0,2) errors	$3.6 \pm 1.9 \text{ mm yr}^{-1}$ pseudo- $r^2 = 0.25$ p = 0.063 ARIMA (1,0,2) errors



Wetlands Page 9 of 17 8

average 29 times per month between May and August. The average flooding duration in 2019 was 2.6 ± 1.1 h, and the marsh flooded on average to a depth of 12 ± 8.8 cm. While marsh flooding was limited to spring tides during both time periods, high tides resulted in marsh flooding about 2.4 times more frequently in 2019 than 1999.

The groundwater table at Piermont Marsh was found to vary with distance from the creek. The low tide water level was lower below the marsh surface and experienced more variability adjacent to tidal creeks (Figs. 5–7). In contrast, the water table was more invariant and had a higher mean position in the marsh interior. (Figs. 5–7; Tables S1–S7, Supplemental material). Comparing low and high tide water

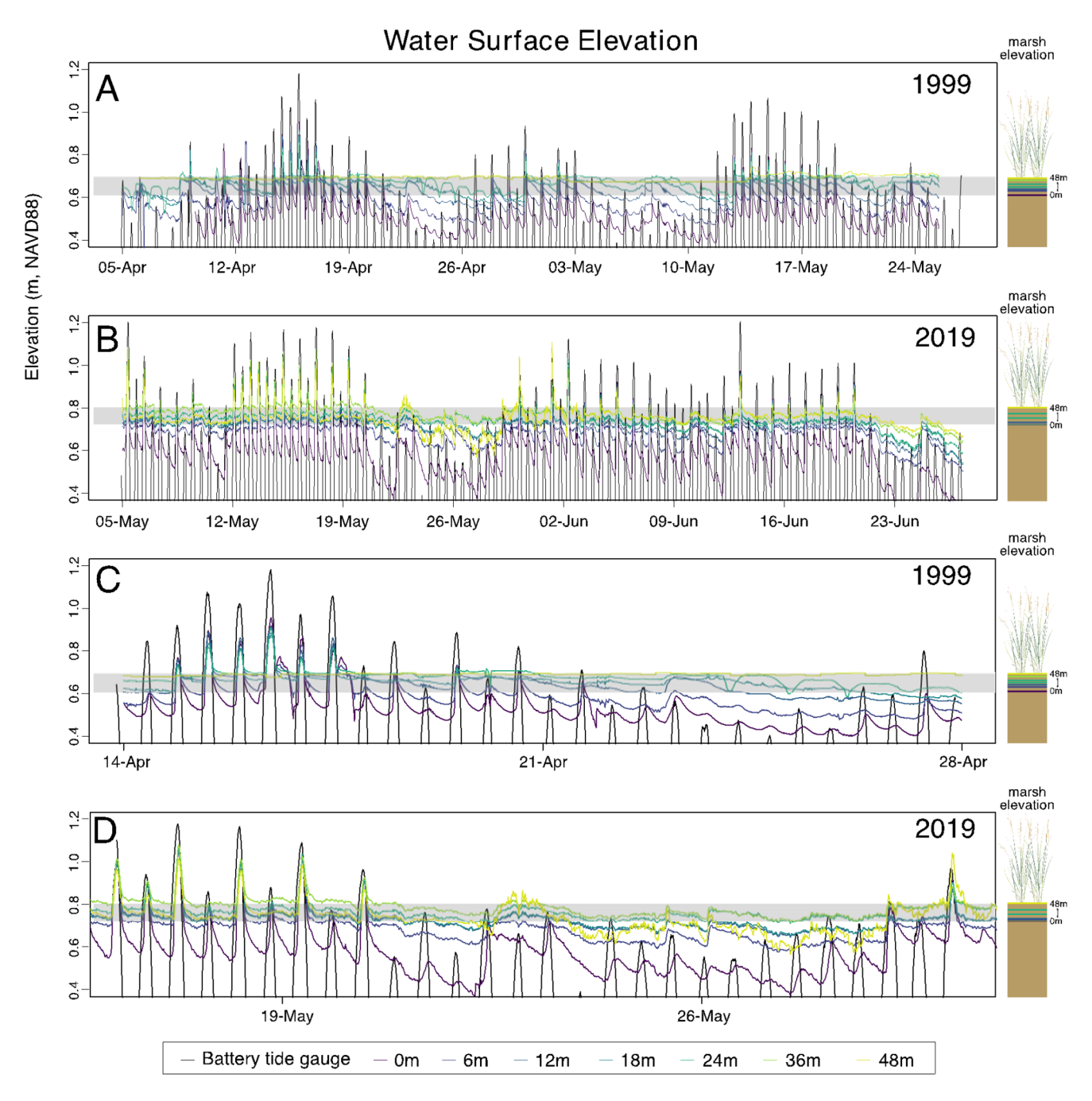


Fig. 5 Water surface elevations across the full study period Piermont Marsh (a) 1999 and (b) 2019 (c) and 14-day periods including both spring and neap tides for (c) 1999 and (d) 2019. Tidal signal from the NOAA Battery gauge (~55 km away) is shown in black (NOAA 2023), and each Piermont Marsh well is represented by a gradient from

yellow to purple. Yellows are further from the tidal creek and purples are closer to the creek. The range of marsh elevations found along the transect are shown in grey. The elevations of individual stations are shown at right. There is a gradient of lower elevations found channel-side and higher elevations in the marsh interior



8 Page 10 of 17 Wetlands

Mean high and low tides relative to the marsh surface

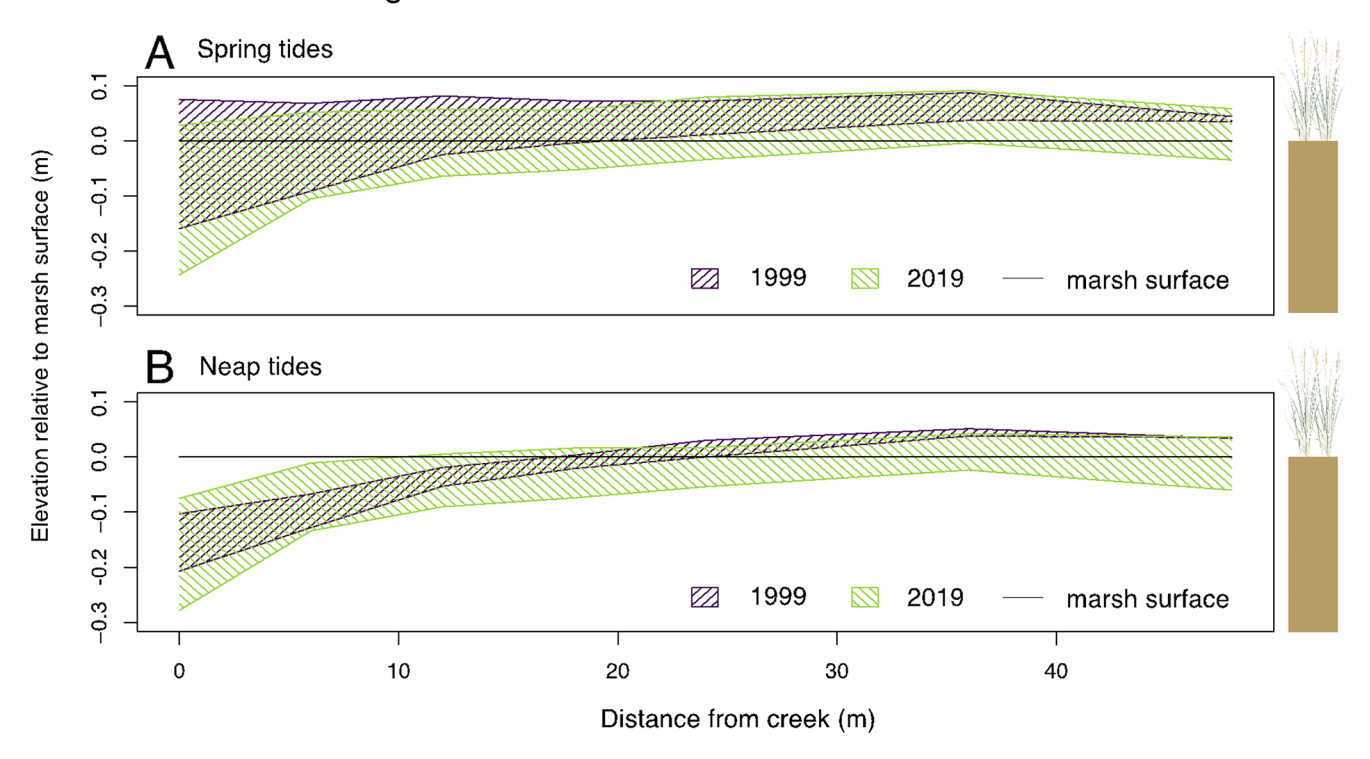


Fig. 6 Mean water surface elevations at minimum low tide and maximum high tide across a transect perpendicular to a large tidal channel during (a) spring and (b) neap tidal cycles in spring 1999 and 2019

levels during 1999 and 2019 revealed some significant differences. Relative to the NAVD88 datum, low tide water levels were on average 7-cm higher in 2019 than in 1999 (Tables S1 and S2). Low tide water levels were on average further below the marsh surface in 2019 than in 1999 (2 cm lower during spring tides, 4 cm lower during neap tides) (Tables S3 and S4, Supplemental Material). In addition, low tide water levels were less variant in 1999 than 2019 at the marsh edge (stations 0-m, 6 m) and in the marsh interior (stations 36-m, 48 m) (Tables S5 and S6, Supplemental material). The low tide standard deviation was 4-cm greater in 2019 than 1999 during neap tides and 2-cm during spring tides.

Relative to the NAVD88 datum, high tide water levels measured in wells were on average 12-cm higher in 2019 than in 1999, 13-cm greater during neap tides and 11-cm greater during neap tides (Fig. 7; Tables S7and S8, Supplemental Material). In contrast, neap tides were 4-cm higher relative to the marsh surface in 2019 than in 1999 (Table S9, Supplemental material) and spring tide water levels were at a similar elevation (1-cm higher) (Table S10, Supplemental material). Neap high tide water levels had a greater standard deviation (7 cm) in 2019, while there was no significant difference for spring tides (Fig. 7; Tables S11 and S12, Supplemental Material).

Tidal efficiency, as a metric that integrates changes in both low and high tide water levels, was found to increase between 1999 and 2019. On average the amount of the fraction of tidal range observed at the tide station that was apparent in the wells increased from 0.060 to 0.12, an increase of 246%. The fraction of tidal efficiency increase was greater adjacent to the tidal channel (e.g., from 0.15 to 0.23, an increase of 0.53 or 53%, at 0-m). However, the relative increase was greater at the more inland sights (e.g., from 0.0062 to 0.078, a 1150% increase at 48-m) (Table 3).

Error and Uncertainty

Results suggested that relative to the NAVD88 datum, low tide water levels measured in wells were 7-cm greater in 2019 than in 1999, and high tide water levels were 12-cm greater in 2019 than 1999. Uncertainty from GPS measurement error, pressure loggers, and conversions between the NGVD29 toNAVD88 datum sum to an estimate of ±3.5 cm using error propagation techniques for independent errors. Thus, these finds are resilient to such uncertainties. However, we estimate that that low tide water levels were further 3-cm below the marsh surface in 2019 than in 1999, and that neap high tides were 4-cm higher relative to the marsh surface in 2019. These measurements are less clearly significant relative to uncertainty estimates. However, measures



Wetlands Page 11 of 17 8

Low tide water surface elevation vs. distance from creek

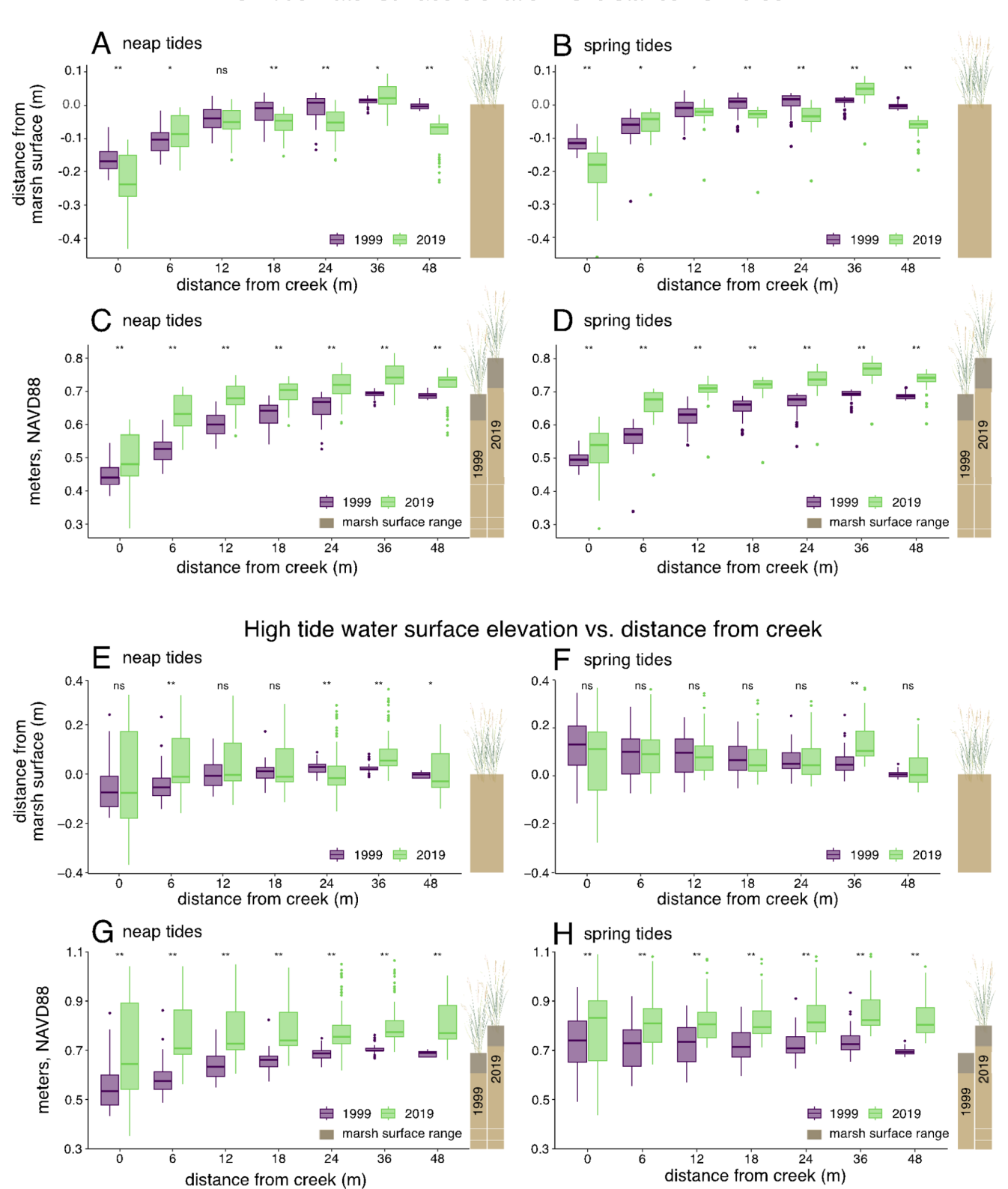


Fig. 7 Box plots depicting the median (line), lower and upper quartiles (box edges), and distribution (whiskers, showing 1.5x the inter-quartile ranges), and outliers (points greater and less than 1.5x the IQR) of in the minimum water surface elevation at low tide relative to the

marsh surface (plot a and b) and relative to NAVD88 (plots c and d) during neap and spring cycles in 1999 and 2019 across a transect with increasing distance from a tidal channel



8 Page 12 of 17 Wetlands

Table 3 Tidal efficiency along a transect with increasing distance from a tidal channel platform in 1999 and 2019. Uncertainties are standard deviations

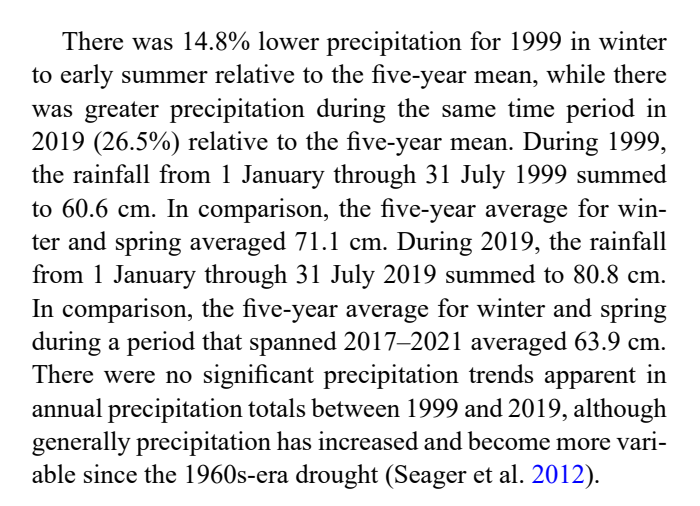
Tidal Efficiency						
Station	1999	2019	Difference			
0-m	0.15 ± 0.078	0.23 ± 0.11	+52.6%			
6-m	0.094 ± 0.083	0.13 ± 0.098	+40.1%			
12-m	0.056 ± 0.060	0.10 ± 0.084	+81.2%			
18-m	0.044 ± 0.052	0.10 ± 0.083	+118%			
24-m	0.042 ± 0.044	0.088 ± 0.078	+108%			
36-m	0.027 ± 0.043	0.077 ± 0.068	+186%			
48-m	0.0062 ± 0.0083	0.078 ± 0.073	+1150%			
average	0.060 ± 0.053	0.12 ± 0.085	+246%			

of variance should not be subject to these uncertainties. Low tide water levels varied less in 1999 than 2019, and high tide water levels varied less in 1999 than 2019 during neap tides, suggesting tidal regime shifts that are apparent despite measurement errors.

The log well time constant was estimated at 1.2 s, which is slightly higher than ideal (1.0 s), but lower than all the measures reported by Gardner (2009) which encompass a range of screened intervals and marsh soil hydraulic conductivities. Thus, these results suggest only minor deviations between measured and actual aquifer head.

Representativeness of Study Periods

A comparison of mean monthly high water and mean sea level in April and May vs. May and June at the Battery tide gauge, suggests that on average MHW is 1.9-cm higher, and MSL is 1.8-cm higher in May-June than April-May (Fig. 7). Thus, we feel that our comparison of April-May vs. May-June contains a modest but not large artifact. A comparison of MHW at the Battery during April-June of 1997-2001 and 2017–2021 found that conditions during 1999 were slightly lower than the five-year mean (0.66 m vs. 0.68 m NAVD88). Conditions in 2019 were slightly above the five-year mean (0.77 m vs. 0.76 m NAVD88) (Fig. 8). Examination of water levels at the Battery shows that measures (in spring 1999) and 2019) occurred during normal and not anomalous tidal periods, although the 2019 sampling took place closer to an astronomical peak or positive deviation in sea level (Fig. 8A) and C). Although we assumed that positioning the sampling periods 20 years apart would mean that we were sampling roughly at the same point in the 18.6 year lunar nodal cycle, there appear to be shorter term cycles (e.g., a 4.4 year subharmonic of the 8.85 year lunar perigee cycle) (Haigh et al., 2011) or periods of positive and negative sea level anomalies that emerge as a combination of the temporal autocorrelation present in water level data (Foster and Brown 2015) (Fig. 8).



Discussion

Hydrology has changed in Piermont Marsh over the last 20 years. Tidal range has increased both in the marsh and at the Battery tide gauge in the Hudson River, and tidal influence extended farther into the marsh in 2019 than in 1999. Mean sea level and marsh elevation have risen at similar rates, at around 5 mm yr⁻¹, but the frequency and magnitude of high water flooding the marsh has increased, which is likely driving changes in hydrology and thus the ecological zonation of marsh habitats. While marsh flooding has increased over time, the water table at many wells was either similar to that found in 1999 or lower relative to the marsh surface at low tide. In addition to SLR, the coverage of P. australis has expanded since 1999 into the marsh interior, which could be a factor in in shaping altering soil porosity, hydraulic conductivity, and evapotranspiration rates, although there is no way to tell from current evidence. It appears that there has been minimal directional change in precipitation, which would affect the runoff or shallow underflows. However, it is worth noting that that there has been an increase in precipitation and its interannual variability in New York City area since the 1960s (Seager et al. 2012).

At Piermont Marsh, it appears that the high tide is increasing at a faster rate than the low tide, and this appears to be reflected in both tide gauge measurements at the Battery tide gauge in NYC, and water table measurements made at Piermont Marsh. For example, low tide water levels measured in wells were 7-cm greater in 2019 than in 1999, and high tide water levels were 12-cm greater in 2019 than 1999 (Supplemental Material). At the Battery tide gauge in NYC, we estimate an increase of 8.2 mm yr⁻¹ in MHW, but an increase of only 3.1 mm yr⁻¹ of MLW. Over a period of 20 years, this suggests that the tide range has expanded by 10.2 cm. While the reason for this shift is not clear (Haigh et al. 2020), increasing tidal ranges introduce more hydraulic



Wetlands Page 13 of 17 8

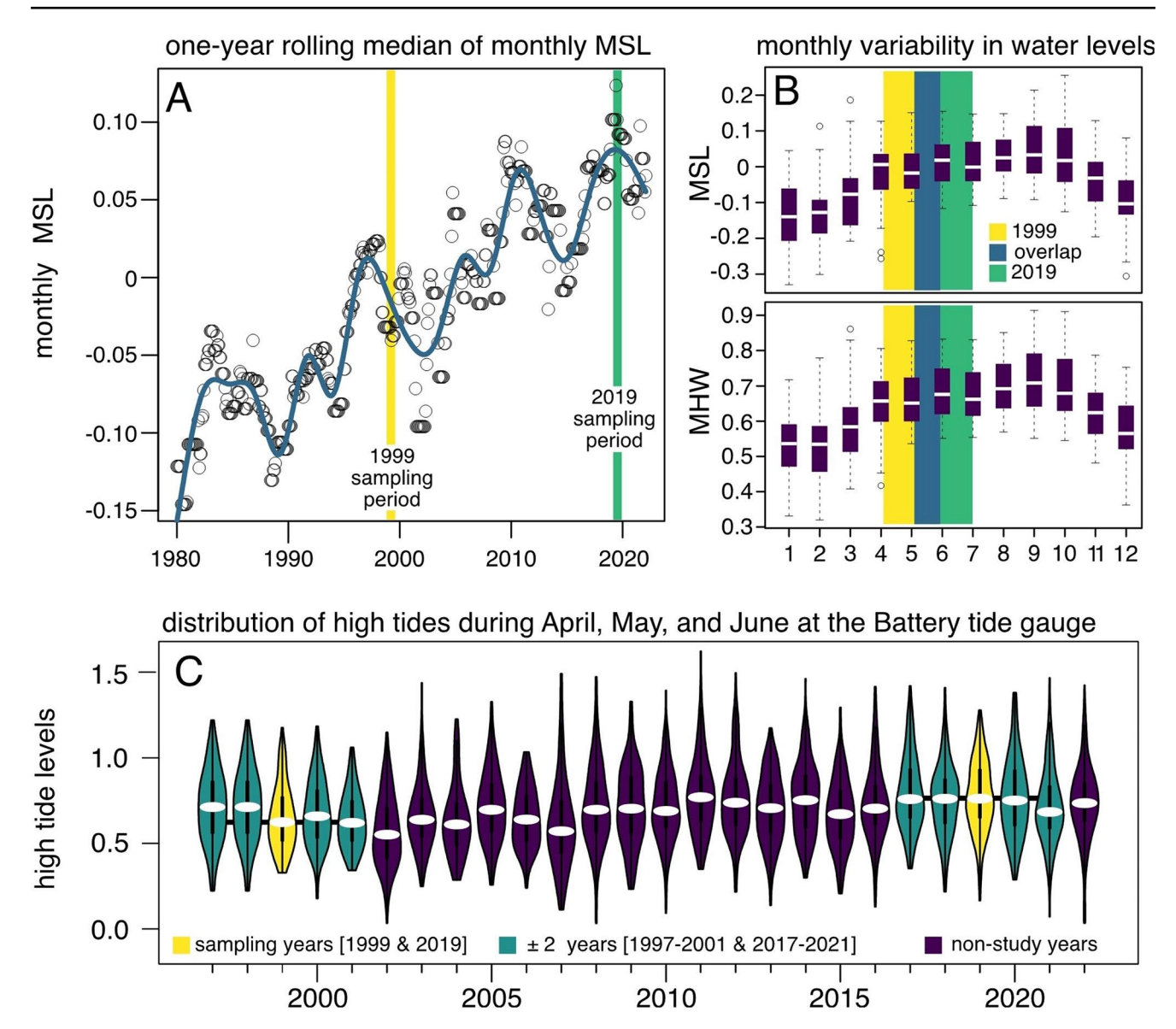


Fig. 8 (a) One year rolling median of monthly mean sea level relative to the NAVD88 datum at the Battery tide gauge (NOAA 2023), with a natural spline used to capture astronomic cycles and upward trends reflected in the tide data (df=16), which may include the 18.6 year nodal cycle, a 8.85 apogee-perigee cycle, and 9.3 and 4.4 year subhar-

monics, (**b**) monthly averages of MSL and MHW at the Battery tide gauge (1980–2022), with circles shown as outliers if they are outside the interquartile range, and (**c**) violin plots of high tides at the Battery during April-May-June from 1997–2022

energy in tidal creeks, which can result in deeper channels with steeper banks (Allen 2000; Williams et al. 2002; Williams and Orr 2002). This creek geometry increases the tidal gradient to the marsh interior, resulting in greater tidal influence on the marsh water table (Mazda and Ikeda 2006).

Increased tidal range driven by higher high tides are contributing to another major trend observed in this study, which is increased tidal influence on the marsh groundwater table, particularly in the marsh interior. In 1999, tidal influence did not propagate more than 20 m into the marsh but in 2019 tidal influence continued far into the marsh interior. In 1999, mean tidal efficiencies at the stations furtherst

from the tidal channel are 0.015. In 2019 tidal efficiencies increased to 0.05 at this station. Because of the change in tidal range and increased tidal efficiency in the marsh interior, the relatively high water table elevations present in 1999 in the marsh interior were less apparent in 2019. This is because in 1999, only the highest tides were propagating into the marsh interior, which caused the mean to increase due to lack of influence from low tides. In 2019, more tides of all magnitudes are propagating into the marsh interior, causing the mean maximum tide to be consistent across the entire transect; however, the mean minimum tides increase in magnitude with distance from the creek both in 1999 and



in 2019, resulting in a high water table in the marsh interior in both years.

As the frequency and magnitude of water table fluctuations determine the eco-hydrological zonation of marsh macrophyte habitat (Moffett et al. 2012; Xin et al. 2013; Wilson et al. 2015b), the observed changes in hydrology are likely altering plant communities across the marsh. Another potential factor is the expansion of P. australis into the marsh interior, which was observed to change in cover at the transect studied at Piermont Marsh between 1999 and 2018. P. australis could have a compounding impact on changes in marsh macrophyte community distribution, because not only does it crowd out native competitors, but dense P. australis populations also alter groundwater hydrology (Windham and Lathrop 1999; Chambers et al. 2003). While there is not extensive research on the impact of P. australis on groundwater hydrology, there is evidence that the P. australis root mat generally increases hydraulic conductivity in marsh sediments (Baird et al. 2004; Saaltink et al. 2019) and that the presence of extensive stands of P. australis can lower the water table due to increased evapotranspiration (Windham and Lathrop 1999; Windham 2001). Although we can't draw any conclusions about the impact of P. australis expansion on the marsh hydrology, it was notable that cover of native grasses increased after Superstorm Sandy led to large areas of plant dieback in 2012 (Fig. 4).

These results were somewhat unexpected in that we anticipated that accelerated sea level rise might be causing increased water table elevations leading to poor drainage. Across the Northeastern US, there are widespread observations of high marsh vegetation dieback that might be expected to result from increased water logging (Watson et al. 2017; Krause et al. 2023), including at Piermont Marsh (Courtney et al. 2020). Rather, we found that even though the elevation of high tides increased significantly, the low tide water table heights were at a similar level as 1999 or lower below the marsh surface in 2019, which we presume is due to the combination of marsh elevation gains keeping pace with sea level rise, possibly in combination with *P. australis* expansion, which may be expected to increase soil hydraulic conductivity. These results point to the importance of strong interactions between marsh vegetation and the marsh water table in the context of climate change. While previous research has strongly demonstrated the role of plant patches in salt marshes creating patterns of eco-hydrologic zonation and geochemical function in through varied evapotranspiration rates and soil rooting depths (Moffett et al. 2012), the implications of this coupling in light of climate change have not been fully realized. Plant evapotranspiration rates are known to vary, but can sum to several cm a day (Borin et al. 2011), in an environment where the water tables often sit within 5-10 cm of the marsh surface. Where plant stress

due to high inundation depresses evapotranspiration, marsh water tables may become even more saturated, and thereby exacerbate the effects of excessive inundation. Conversely, plants supporting high evapotranspiration rates, such as *P. australis* or the tall growth form of *Spartina alterniflora* found in macrotidal salt marshes (Valiela et al. 1978), may be less sensitive to excessive inundation.

A second finding of our study is that tidal range has appeared to increase over the past 20 years at the Battery tide gauge, in NYC, with monthly highest water and monthly average high tide levels rising at faster rates than mean sea level. Other studies have found similar trends globally and locally (Pickering et al. 2012, 2017; Mawdsley et al. 2014; Balke et al. 2016; Talke et al. 2018) and some tidal datums have been updated to reflect changing tidal dynamics due to accelerated SLR (Bamford 2013; Wang and Myers 2016); however, a comprehensive review of mean high water and mean low water trends in the United States has not been published since 2003 (Flick et al. 2003). A more comprehensive analysis of regional tidal range and SLR should be performed to understand changing tidal dynamics in the Mid-Atlantic region and to inform coastal management into the future.

Supplementary Information The online version contains supplementary material available at https://doi.org/10.1007/s13157-023-01761-9.

Acknowledgements This work was supported by a Polgar Grant, awarded to Sofi Courtney by the Hudson River Foundation, and by the National Science Foundation under Grant No. 1946302. We acknowledge Lena Champlin, Johannes Krause, Malakai Madden, Nicolo Montalto, and Iggy for assistance with fieldwork, Patrick Gurian, Kirk Raper, and ChatGPT for data analysis guidance, Michael and Liz Biddle for housing, Sarah Fernald of the HRNERR who assisted with research permits, and Michael Ferrin for overall support.

Author Contributions All authors contributed to the study conception and design. Sofi Courtney led 2019 field data collection, while Franco Montalto led 1999 data collection and processing. Data analysis of groundwater data was performed by Sofi Courtney, and GIS analysis and tide gauge data was analyzed by Elizabeth Watson. The first draft of the manuscript was written by Sofi Courtney and Elizabeth Watson. All authors read and approved the final manuscript.

Funding This work was supported by a Polgar Grant, awarded to Sofi Courtney by the Hudson River Foundation, and by the National Science Foundation under Grant No. 1946302.

Data Availability The datasets generated by this current study, including reproducible R code, are available via the Dryad Digital repository, https://doi.org/10.5061/dryad.cjsxksncr.

Declarations

Competing Interests The authors have no relevant financial or nonfinancial interests to disclose.



Wetlands Page 15 of 17 8

References

- Adler D, Kelly ST, Elliott T, Adamson J (2022) vioplot: violin plot. R package version 0.4.0
- Ahlmann-Eltze C, Patil I (2021) Ggsignif: R Package for displaying significance brackets for ggplot2. https://doi.org/10.31234/osf.io/7awm6
- Allen J (2000) Morphodynamics of Holocene salt marshes: a review sketch from the Atlantic and Southern North Sea coasts of Europe. Q Sci Rev 19:1155–1231. https://doi.org/10.1016/S0277-3791(99)00034-7
- Anda A, Soos G, da Teixeira JA (2017) Practical use of Phragmites australis to study evapotranspiration in a wetland zone of Lake Balaton (Southwest Hungary). 127:899–909Theoretical and applied climatology
- Baird AJ, Surridge BWJ, Money RP (2004) An assessment of the piezometer method for measuring the hydraulic conductivity of *Cladium mariscus*—Phragmites australis root mat in a Norfolk(UK) Fen. Hydrol Process 18:275–291. https://doi. org/10.1002/hyp.1375
- Balke T, Stock M, Jensen K et al (2016) A global analysis of the seaward salt marsh extent: the importance of tidal range: THE GLOBAL SEAWARD SALT MARSH EXTENT. Water Resour Res 52:3775–3786. https://doi.org/10.1002/2015WR018318
- Bamford HA (2013) Notice of change to the Nation's tidal datums with the adoption of a Modified Procedure for Computation of Tidal Datums in Area of Anomalous Sea-Level Change
- Bates DM, Venables W (2023) Regression Spline Functions and Classes. https://r-universe.dev/manuals/splines.html
- Borin M, Milani M, Salvato M, Toscano A (2011) Evaluation of Phragmites australis (Cav.) Trin. Evapotranspiration in Northern and Southern Italy. Ecol Eng 37:721–728. https://doi.org/10.1016/j.ecoleng.2010.05.003
- Burba GG, Verma SB, Kim J (1999) Surface energy fluxes of Phragmites australis in a prairie wetland. Agric for Meteorol 94(1):31-51
- Cao M, Xin P, Jin G, Li L (2012) A field study on groundwater dynamics in a salt marsh Chongming Dongtan wetland. Ecol Eng 40:61–69. https://doi.org/10.1016/j.ecoleng.2011.12.018
- Chambers RM, Osgood DT, Bart DJ, Montalto F (2003) Phragmites australis invasion and expansion in tidal wetlands: interactions among salinity, sulfide, and hydrology. Estuaries 26:398–406. https://doi.org/10.1007/BF02823716
- Charette MA (2007) Hydrologic forcing of submarine groundwater discharge: insight from a seasonal study of radium isotopes in a groundwater-dominated salt marsh estuary. Limnol Oceanogr 52:230–239. https://doi.org/10.4319/lo.2007.52.1.0230
- Chui TFM, Low SY, Liong S-Y (2011) An ecohydrological model for studying groundwater-vegetation interactions in wetlands. J Hydrol 409:291–304. https://doi.org/10.1016/j.jhydrol.2011.08.039
- Cole Ekberg ML, Raposa KB, Ferguson WS et al (2017) Development and application of a method to identify Salt Marsh vulnerability to sea level rise. Estuaries Coasts 40:694–710. https://doi.org/10.1007/s12237-017-0219-0
- Courtney S, Montalto F, Watson E (2020) Is sea level rise altering wetland hydrology in hudson river valley tidal marshes? Final reports of the Tibor T. Polgar fellowship program. Hudson River Foundation, pp 1–36
- D'Alpaos A, Marani M (2016) Reading the signatures of biologic—geomorphic feedbacks in salt-marsh landscapes. Adv Water Resour 93:265–275. https://doi.org/10.1016/j.advwatres.2015.09.004
- Dacey JWH, Howes BL (1984) Water uptake by Roots Controls Water Table Movement and Sediment Oxidation in Short

- Spartina Marsh. Science 224:487–489. https://doi.org/10.1126/science.224.4648.487
- DeLaune RD, Smith CJ, Patrick WH (1983) Relationship of Marsh Elevation, Redox Potential, and Sulfide to Spartina alterniflora Productivity. Soil Sci Soc Am J 47:930–935. https://doi.org/10.2136/sssaj1983.03615995004700050018x
- Elsey-Quirk T, Watson EB, Raper K et al (2022) Relationships between ecosystem properties and sea-level rise vulnerability of tidal wetlands of the U.S. Mid-atlantic. Environ Monit Assess 194:292. https://doi.org/10.1007/s10661-022-09949-y
- Ferris JG, Knowles DB, Brown RH, Stallman RW (1962) Theory of Aquifer tests. United States Government Printing Office, Washington DC
- Flick RE, Murray JF, Ewing LC (2003) Trends in United States Tidal Datum statistics and Tide Range. J Waterw Port Coast Ocean Eng 129:155–164 doi: 10.1061/(ASCE)0733-950X(2003)129:4(155)
- Foster G, Brown PT (2015) Time and tide: analysis of sea level time series. Clim Dyn 45:291–308. https://doi.org/10.1007/s00382-014-2224-3
- Gardner LR (2009) Assessing the accuracy of monitoring wells in tidal wetlands. Water Resour Res 45(2). https://doi.org/10.1029/2008WR007626
- Guimond J, Tamborski J (2021) Salt Marsh Hydrogeology: a review. Water 13:543. https://doi.org/10.3390/w13040543
- Guimond JA, Seyfferth AL, Moffett KB, Michael HA (2020a) A physical-biogeochemical mechanism for negative feedback between marsh crabs and carbon storage. Environ Res Lett 15:034024. https://doi.org/10.1088/1748-9326/ab60e2
- Guimond JA, Yu X, Seyfferth AL, Michael HA (2020b) Using hydrological-biogeochemical linkages to Elucidate Carbon Dynamics in Coastal marshes subject to relative sea level rise. Water Resour Res. https://doi.org/10.1029/2019WR026302
- Haigh ID, Pickering MD, Green JM, Arbic BK, Arns A, Dangendorf S, Hill DF, Horsburgh K, Howard T, Idier D, Jay DA (2020) The tides they are a-Changin': a comprehensive review of past and future nonastronomical changes in tides, their driving mechanisms, and future implications. Rev Geophys 58(1):e2018RG000636
- Harvey JW, Odum WE (1990) The influence of tidal marshes on upland groundwater discharge to estuaries. Biogeochemistry 10:217–236. https://doi.org/10.1007/BF00003145
- Headley TR, Davison L, Huett DO, Müller R (2012) Evapotranspiration from subsurface horizontal flow wetlands planted with Phragmites australis in sub-tropical Australia. Water Res 46(2):345–354
- Hughes ALH, Wilson AM, Morris JT (2012) Hydrologic variability in a salt marsh: Assessing the links between drought and acute marsh dieback. Estuarine, Coastal and Shelf Science 111:95–106. https://doi.org/10.1016/j.ecss.2012.06.016
- Hyndman RJ, Khandakar Y (2008) Automatic Time Series forecasting: the forecast Package for R. J Stat Softw. https://doi.org/10.18637/ iss v027.i03
- Jiao J, and V. Post (2019) Coastal Hydrogeology. Cambridge University Press, Cambridge, UK, p 419
- Kassambara A (2023) Ggpubr: ggplot2. Based Publication Ready Plots Knott JF, Jacobs JM, Daniel JS, Kirshen P (2019) Modeling Groundwater rise caused by sea-level rise in Coastal New Hampshire. J Coastal Res 35:143. https://doi.org/10.2112/JCOASTRES-D-17-00153.1
- Krause JR, Oczkowski AJ, Watson EB (2023) Improved mapping of coastal salt marsh habitat change at Barnegat Bay (NJ, USA) using object-based image analysis of high-resolution aerial imagery. Remote Sens Applications: Soc Environ 29:100910. https:// doi.org/10.1016/j.rsase.2022.100910
- Lathrop RG, Windham L, Montesano P (2003) Does Phragmites expansion alter the structure and function of marsh landscapes?



- Patterns and processes revisited. Estuaries 26:423–435. https://doi.org/10.1007/BF02823719
- Mawdsley RJ, Haigh ID, Wells NC (2014) Global changes in mean tidal high water, low water and range. J Coastal Res 70:343–348. https://doi.org/10.2112/SI70-058.1
- Mazda Y, Ikeda Y (2006) Behavior of the groundwater in a riverinetype mangrove forest. Wetlands Ecol Manage 14:477–488
- Mendelssohn IA, McKee KL (1988) Spartina Alterniflora Die-Back in Louisiana: Time-Course Investigation of Soil Waterlogging effects. J Ecol 76:509. https://doi.org/10.2307/2260609
- Milani M, Toscano A (2013) Evapotranspiration from pilot-scale constructed wetlands planted with *Phragmites australis* in a Mediterranean environment. J Environ Sci Health Part A 48:568–580. https://doi.org/10.1080/10934529.2013.730457
- Moffett KB, Gorelick SM (2016) Relating salt marsh pore water geochemistry patterns to vegetation zones and hydrologic influences. Water Resour Res 52:1729–1745. https://doi.org/10.1002/2015WR017406
- Moffett KB, Gorelick SM, McLaren RG, Sudicky EA (2012) Salt marsh ecohydrological zonation due to heterogeneous vegetationgroundwater-surface water interactions: SALT MARSH ECO-HYDROLOGICAL ZONATION MODELING. Water Resour Res. https://doi.org/10.1029/2011WR010874
- Montalto FA, Steenhuis TS (2004) The link between hydrology and restoration of tidal marshes in the New York/ New Jersey Estuary. Wetlands 24:414–425. https://doi. org/10.1672/0277-5212(2004)024[0414:TLBHAR]2.0.CO;2
- Montalto FA, Steenhuis TS, Parlange J-Y (2006) The hydrology of Piermont Marsh, a reference for tidal marsh restoration in the Hudson river estuary, New York. J Hydrol 316:108–128. https://doi.org/10.1016/j.jhydrol.2005.03.043
- Morris J, Sundberg KL, Hopkinson C (2013) Salt Marsh Primary Production and its responses to relative sea level and nutrients in estuaries at Plum Island, Massachusetts, and North Inlet, South Carolina, USA. Oceanography 26:78–84
- Mulcare DM, NGS Toolkit, Part 9: The National Geodetic Survey VERTCON Tool., See (2004) https://www.ngs.noaa.gov/TOOLS/Professional Surveyor Articles/VERTCON.pdf
- NCEI (2023) Local Climatological Data. Westchester Co. Airport, NY, USA. station ID WBAN94745
- NERRS (2019) Centralized Data Management Office
- NOAA (2023) 8518750 the Battery, NY, Tides/Water levels. Center for Operational Oceanographic Products and Services
- NOAA (2019) Vertical Datum Transformation: Integrating America's Elevation Data
- Nuttle WK, Hemand HF (1988) Salt marsh hydrology: implications for biogeochemical fluxes to the atmosphere and estuaries. Glob Biogeochem Cycles 2:91–114. https://doi.org/10.1029/GB002i002p00091
- NYDOS (2012) Coastal Fish and Wildlife Rating Form
- NYSDEC (2017) Draft Piermont Marsh Reserve Management Plan
- NYSDEC (1985) Piermont Pier Critical Environmental Area
- NYSDEC (2023) Hudson River Estuary tidal wetlands. Vegetation maps created for 1997, 2005, 2014, and 2018
- Ogle DH, Doll JC, Powell Wheeler A, Dinno A (2023) FSA: Simple Fisheries Stock Assessment Methods. R package version 0.9.4
- Osborne RI, Bernot MJ, Findlay SE (2015) Changes in nitrogen cycling processes along a salinity gradient in tidal wetlands of the Hudson River, New York, USA. *Wetlands*, 35, 323–334
- Pickering MD, Wells NC, Horsburgh KJ, Green JAM (2012) The impact of future sea-level rise on the European Shelf tides. Cont Shelf Res 35:1–15. https://doi.org/10.1016/j.csr.2011.11.011
- Pickering MD, Horsburgh KJ, Blundell JR et al (2017) The impact of future sea-level rise on the global tides. Cont Shelf Res 142:50–68. https://doi.org/10.1016/j.csr.2017.02.004

- R Core Team (2022) R: A language and environment for statistical computing
- Raposa KB, Wasson K, Smith E et al (2016) Assessing tidal marsh resilience to sea-level rise at broad geographic scales with multi-metric indices. Biol Conserv 204:263–275. https://doi.org/10.1016/j.biocon.2016.10.015
- Raposa KB, Weber RLJ, Ekberg MC, Ferguson W (2017) Vegetation dynamics in Rhode Island Salt marshes during a period of accelerating sea level rise and Extreme Sea Level events. Estuaries Coasts 40:640–650. https://doi.org/10.1007/s12237-015-0018-4
- Rippel TM, Minsavage-Davis CD, Shirey V, Wimp GM (2023) Simple machine learning with aerial imagery reveals severe loss of a salt Marsh Foundation species. Estuaries Coasts 46:1110–1122. https://doi.org/10.1007/s12237-023-01192-z
- Saaltink RM, Barciela-Rial M, Van Kessel T, et al (2019) Drainage of soft cohesive sediment with and without *Phragmites australis* as an ecological engineer. doi: 10.5194/hess-2019-194
- Sanderson EW, Ustin SL, Foin TC (2000) The influence of tidal channels on the distribution of salt marsh plant species in Petaluma Marsh, CA, USA. Plant Ecol 146:29–41. https://doi.org/10.1023/A:1009882110988
- Schepers L, Brennand P, Kirwan ML et al (2020) Coastal Marsh Degradation into ponds induces irreversible elevation loss relative to Sea Level in a Microtidal System. Geophys Res Lett. https://doi.org/10.1029/2020GL089121
- Seager R, Pederson N, Kushnir Y, Nakamura J, Jurburg S (2012) The 1960s drought and the subsequent shift to a wetter climate in the Catskill Mountains region of the New York City watershed. J Clim 25(19):6721–6742
- Shi X, Benitez-Nelson CR, Cai P et al (2019) Development of a two-layer transport model in layered muddy–permeable marsh sediments using ²²⁴ Ra– ²²⁸ th disequilibria. Limnol Oceanogr 64:1672–1687. https://doi.org/10.1002/lno.11143
- Smith SM (2015) Vegetation change in Salt marshes of Cape Cod National Seashore (Massachusetts, USA) between 1984 and 2013. Wetlands 35:127–136. https://doi.org/10.1007/s13157-014-0601-7
- Smith S, Medeiros K (2013) Manipulation of water levels to facilitate Vegetation Change in a Coastal lagoon undergoing partial tidal restoration (Cape Cod, Massachusetts). J Coastal Res 291:93–99. https://doi.org/10.2112/JCOASTRES-D-12-00035.1
- Smith SM, Medeiros KC, Tyrrell MC, Massachusetts USA (2012) J Coastal Res 282:602–612. https://doi.org/10.2112/ JCOASTRES-D-10-00175.1
- Smith SM, Tyrrell MC, Congretel M (2013) Palatability of salt marsh forbs and grasses to the purple marsh crab (Sesarma reticulatum) and the potential for re-vegetation of herbivory-induced salt marsh dieback areas in cape cod (Massachusetts, USA). Wetlands Ecol Manage 21:263–275. https://doi.org/10.1007/s11273-013-9298-2
- Talke SA, Kemp AC, Woodruff J (2018) Relative sea level, tides, and Extreme Water levels in Boston Harbor from 1825 to 2018. J Geophys Research: Oceans 123:3895–3914. https://doi.org/10.1029/2017JC013645
- Tang Y-N, Ma J, Xu J-X et al (2022) Assessing the impacts of tidal creeks on the spatial patterns of Coastal Salt Marsh Vegetation and its Aboveground Biomass. Remote Sens 14:1839. https://doi.org/10.3390/rs14081839
- Taylor JR (1997) An introduction to error analysis: the study of uncertainties in physical measurements, 2nd edn. University Science Books, Sausalito.
- Trapletti A, Hornik K (2023) Tseries: Time Series Analysis and Computational Finance. R Package Version 0:10–54
- Ulrich J (2021) Technical Trading Rules. R package version 0.24.3 Valiela I, Teal J, Deuser W (1978) The nature of growth forms in the salt marsh grass Spartina alterniflora. Am Nat 112:461–470



Wetlands Page 17 of 17

Van der Kamp G (1972) August. Tidal fluctuations in a confined aquifer extending under the sea. International Geological Congress, vol 24. Quebec, Montreal, pp 101–106. 11

- Wang J, Myers E (2016) Tidal Datum Changes Induced by Morphological Changes of North Carolina Coastal Inlets. J Mar Sci Eng 4:79. https://doi.org/10.3390/imse4040079
- Wang X, Li R, Taghadomi HJ et al (2017) Effects of sea level rise on hydrology: case study in a typical mid-atlantic coastal watershed. J Water Clim Change 8:730–754. https://doi.org/10.2166/ wcc.2017.156
- Watson EB, Wigand C, Davey EW et al (2017) Wetland loss patterns and Inundation-Productivity Relationships Prognosticate Widespread Salt Marsh Loss for Southern New England. Estuaries Coasts 40:662–681. https://doi.org/10.1007/s12237-016-0069-1
- Watson EB, Ferguson W, Champlin LK et al (2022) Runnels mitigate marsh drowning in microtidal salt marshes. Front Environ Sci 10:987246. https://doi.org/10.3389/fenvs.2022.987246
- White SM, Madsen EA (2016) Tracking tidal inundation in a coastal salt marsh with Helikite airphotos: influence of hydrology on ecological zonation at Crab Haul Creek, South Carolina. Remote Sens Environ 184:605–614. https://doi.org/10.1016/j.rse.2016.08.005
- Wickham H (2016) ggplot2: Elegant Graphics for Data Analysis, 2nd ed. 2016. https://doi.org/10.1007/978-3-319-24277-4
- Wickham H, François R, Henry L, Müller K (2022) dplyr: A Grammar of Data Manipulation
- Williams PB, Orr MK (2002) Physical evolution of restored breached Levee Salt marshes in the San Francisco Bay Estuary. Restor Ecol 10:527–542. https://doi.org/10.1046/j.1526-100X.2002.02031.x
- Williams PB, Orr MK, Garrity NJ (2002) Hydraulic geometry: a Geomorphic Design Tool for Tidal Marsh Channel evolution in Wetland Restoration projects. Restor Ecol 10:577–590. https://doi.org/10.1046/j.1526-100X.2002.t01-1-02035.x
- Wilson AM, Morris JT (2012) The influence of tidal forcing on ground-water flow and nutrient exchange in a salt marsh-dominated estuary. Biogeochemistry 108:27–38. https://doi.org/10.1007/s10533-010-9570-y
- Wilson AM, Moore WS, Joye SB et al (2011) Storm-driven ground-water flow in a salt marsh. Water Resour Res. https://doi.org/10.1029/2010WR009496
- Wilson AM, Evans T, Moore W et al (2015a) What time scales are important for monitoring tidally-influenced submarine groundwater discharge? Insights from a salt marsh. Water Resour Res 51:4198–4207. https://doi.org/10.1002/2014WR015984
- Wilson AM, Evans T, Moore W et al (2015b) Groundwater controls ecological zonation of salt marsh macrophytes. Ecology 96:840–849. https://doi.org/10.1890/13-2183.1
- Windham L (2001) Comparison of biomass production and decomposition between Phragmites australis (common reed) and Spartina patens (salt hay grass) in brackish tidal marshes of New Jersey, USA. Wetlands 21:179–188. https://doi.org/10.1672/0277-5212(2001)021[0179:COBPAD]2.0.CO;2

- Windham L, Lathrop RG (1999) Effects of Phragmites australis (Common Reed) Invasion on Aboveground Biomass and Soil properties in Brackish Tidal Marsh of the Mullica River, New Jersey. Estuaries 22:927. https://doi.org/10.2307/1353072
- Xie H, Yi Y, Hou C, Yang Z (2020) In situ experiment on groundwater control of the ecological zonation of salt marsh macrophytes in an estuarine area. J Hydrol 585:124844. https://doi.org/10.1016/j.jhydrol.2020.124844
- Xin P, Kong J, Li L, Barry DA (2013) Modelling of groundwater–vegetation interactions in a tidal marsh. Adv Water Resour 57:52–68. https://doi.org/10.1016/j.advwatres.2013.04.005
- Xin P, Zhou T, Lu C et al (2017) Combined effects of tides, evaporation and rainfall on the soil conditions in an intertidal creek-marsh system. Adv Water Resour 103:1–15. https://doi.org/10.1016/j.advwatres.2017.02.014
- Xin P, Wilson A, Shen C et al (2022) Surface Water and Groundwater interactions in Salt marshes and their impact on Plant Ecology and Coastal Biogeochemistry. Rev Geophys. https://doi.org/10.1029/2021RG000740
- Yozzo DJ, Osgood DT (2013) Invertebrate communities of low-salinity wetlands: overview and comparison between Phragmites and Typha marshes within the Hudson River Estuary. Estuaries Coasts 36:575–584. https://doi.org/10.1007/s12237-012-9543-6
- Yue S, Pilon P, Cavadias G (2002) Power of the Mann–Kendall and Spearman's rho tests for detecting monotonic trends in hydrological series. J Hydrol 259:254–271. https://doi.org/10.1016/ S0022-1694(01)00594-7
- Zeileis A (2004) Econometric Computing with HC and HAC Covariance Matrix estimators. J Stat Softw. https://doi.org/10.18637/jss.v011.i10
- Zeileis A, Hothorn T (2002) Diagnostic checking in Regression relationships. R News 2:7–10
- Zeileis A, Köll S, Graham N (2020) Various versatile variances: an object-oriented implementation of clustered covariances in *R*. J Stat Softw. https://doi.org/10.18637/jss.v095.i01
- Zhou L, Zhou G (2009) Measurement and modelling of evapotranspiration over a reed (Phragmites australis) marsh in Northeast China. J Hydrol 372(1–4):41–47

Publisher's Note Springer Nature remains neutral with regard to jurisdictional claims in published maps and institutional affiliations.

Springer Nature or its licensor (e.g. a society or other partner) holds exclusive rights to this article under a publishing agreement with the author(s) or other rightsholder(s); author self-archiving of the accepted manuscript version of this article is solely governed by the terms of such publishing agreement and applicable law.

